Two-wavelength laser diode interferometer with a time-sharing heterodyne modulation

Takamasa Suzuki, Takatsugu Aizaki, Osami Sasaki, and Takeo Maruyama

Niigata University, Faculty of Engineering
8050 Ikarashi 2, Niigata 950-21, Japan

ABSTRACT

A new type of two-wavelength interferometer for the measurement of absolute distance is described. Since the wavelength of the laser diode is temporally multiplexed, only one laser diode light-source is required, thus eliminating the necessity of aligning two independent optical axes. Absolute distance is calculated from the difference of the phases in the interference signals generated by each wavelength. The self-correlation function is applicable in our system for detecting this phase-difference between two kinds of interference signals, thereby, the signal processing is very simple and there is a possibility that the real-time distance measurement becomes possible in our new method.

Keywords: interferometer, laser diode, two-wavelength, equivalent wavelength, absolute distance measurement

1. INTRODUCTION

Optical interferometry provides a highly accurate means of measuring both vibration and surface profile in a manner requiring no physical contact. In addition, recent advances in signal processing have substantially reduced external disturbance and phase unwrapping. The former problem can be removed by controlling the injection current of the laser diode (LD) with a closed loop control system[1-4]. The latter one is settled by means of an appropriate signal processing[5] or a clever optical system. One of the most popular ways to overcome the phase unwrapping is through the use of two-wavelength interferometry. While the concept of the two-wavelength interferometer (TWI) is admittedly not a new one[6], it is in fact very effective, for the measurement of rough surface[7] because large equivalent wavelength can be used.

With so many kinds of LDs having been developed, recently, we have available to use a number of different wavelengths. So the TWI is used to constructed with different two LDs[8-10]. But the alignment of the optical axes for each LD is complicated and stabilization of the relative change of the wavelengths[11] is very difficult in this type of interferometer.

We therefore tried to determine if we could turn the wavelength tunability into an asset rather than a drawback, and proposed a new type of TWI based on a single LD. The LD alternately oscillates within two slightly different wavelengths in this TWI. Consequently, the synthesized equivalent wavelength becomes very large. It is, however, difficult to measure the distance with a high degree of accuracy. So we applied phase-locked LD interferometry[12,13] to boost accuracy, and were then able to measure one-dimensional step-height surface profile accurately[14]. But the control system of that TWI is somewhat complicated.

In this paper, we propose a modulating technique for constructing the TWI for absolute distance measurement. The basic concept of this TWI is the same as a previous one which employed a single LD. It does not require a complicated phase-locked system, but instead uses time-shared heterodyne modulation. In this modulation, the dc level of the injected modulating current is alternates, and the two dc currents determine the two wavelengths of the LD. Absolute distance is then calculated, from the difference in the phases of the interference signals, which are generated by each wavelength. Since the self-correlation function between two interference signals is used to obtain the phase difference, real-time signal processing can be easily achieved.

SPIE Vol. 2993 • 0277-786X/97/$10.00

In Sec. 2, we describe the basic configuration of this interferometer, the principle of phase detection, and absolute distance measurement. The experimental setup and results are presented in Sec. 3 and Sec. 4, respectively.

2. PRINCIPLE

The configuration of our interferometer is shown in Fig. 1. The light from the LD is collimated with lens L and is led to the Twyman-Green interferometer which consists of a beam splitter (BS), mirrors (M1) and (M2), a pin hole (PH), and a photodetector (PD). The optical path difference (OPD) of the interferometer is given as $2D_0$. A dc bias current I_0, and a modulation current $I_m(t)$ that is generated by the modulation signal generator (MSG) are injected to the LD, through the LD modulator (LM). The MSG also generates a sampling pulse (SP) for the A/D converter. The detected interference signal is processed by computer (PC).

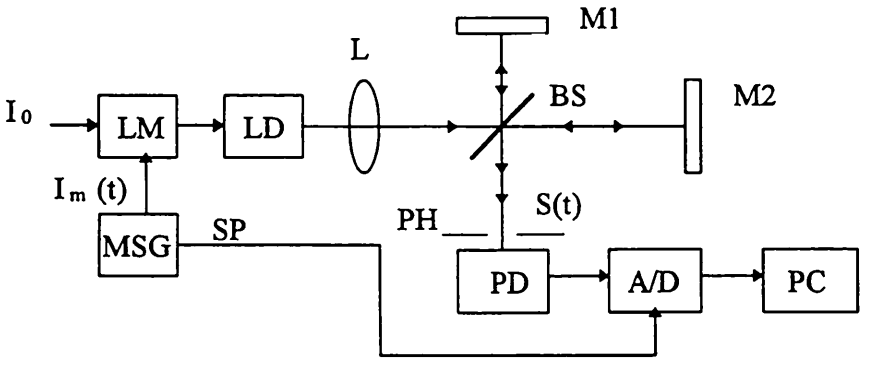

Fig. 1 Experimental setup

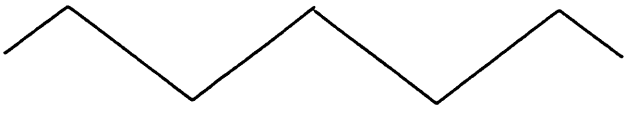

(a) Normal signal

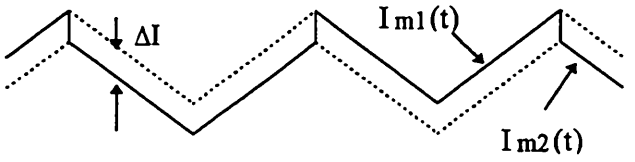

(b) Time-shared signal

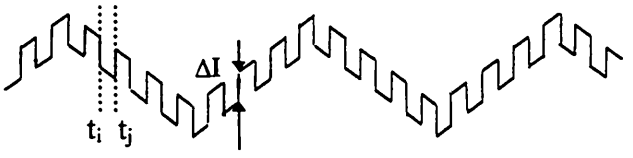

(c) High-speed time-shared signal

Fig. 2 Wave form of the modulating signal

The dc bias current I_0 determines the central wavelength λ_0 of the LD. In our experiments, we used several heterodyne modulating currents shown in Fig. 2, where the inclination of the triangular current is *a* or *-a*. A commonly used normal heterodyne modulating current is shown in Fig. 2(a). If the dc bias current ΔI is superimposed on the heterodyne modulating current for one alternate period, we can obtain the time-shared modulating current, as shown in Fig. 2(b). Moreover, the section for the superimpose of the dc bias current is much shorter than one period, high-speed time-shared modulating current is obtained as shown in Fig. 2(c).

To simplify the explanation, we use the modulating current shown in Fig. 2(b). If we take note of the positive inclination of the modulating current and assume that the dc level of $I_{m1}(t)$ is larger than that of $I_{m2}(t)$ by ΔI, the two modulating currents are represented by

$$I_{m1}(t)=at, \tag{1}$$

and

$$I_{m2}(t)= \Delta I+at, \tag{2}$$

respectively. Then, the ac components of the sinusoidal interference signals

$$S_1(t)=A_1\cos[\omega_{c1}t+\alpha_1], \tag{3}$$

and

$$S_2(t)=A_2\cos[\omega_{c2}t+\alpha_2], \tag{4}$$

are obtained, where

$$\alpha_1 = \frac{4\pi D_0}{\lambda_0}, \tag{5}$$

and

$$\alpha_2 = \frac{4\pi D_0}{\lambda_0 + \Delta\lambda} = \frac{4\pi D_0}{\lambda_0} - \frac{4\pi D_0}{\lambda_0^2}\Delta\lambda, \tag{6}$$

are initial phases in the interference signals, where $\Delta\lambda=\beta\Delta I$, and β is a modulation efficiency of the LD. Phases α_1 and α_2 are determined by the OPD, and $\Delta\lambda$ the difference of the wavelength. The angular frequencies are represented by

$$\omega_{c1} = \frac{4\pi a\beta D_0}{\lambda_0^2}, \tag{7}$$

and

$$\omega_{c2} = \frac{4\pi a\beta D_0}{(\lambda_0 + \Delta\lambda)^2} = \frac{4\pi a\beta D_0}{\lambda_0^2}\left(1 - \frac{\Delta\lambda}{\lambda_0}\right)^2. \tag{8}$$

Coefficient $(1- \Delta\lambda/\lambda_0)^2$ is almost unity, then the approximation of $\omega_{c1}=\omega_{c2}$ is held. The phase difference $\Delta\alpha$ is therefore given by

$$\Delta\alpha = \alpha_1 - \alpha_2 = \frac{4\pi D_0\beta}{\lambda_0^2}\Delta I. \tag{9}$$

The absolute distance D_0 is then given by

$$D_0 = \frac{\lambda_0^2}{4\pi\beta\Delta I}\Delta\alpha . \qquad (10)$$

Equation (10) shows that we have only to measure the phase difference $\Delta\alpha$ between the sinusoidal signals $S_1(t)$ and $S_2(t)$. The phase difference of the sinusoidal signals is obtained easily by using a self-correlation function

$$\rho = \int_{-T/2}^{T/2} S_1(t) \times S_2(t)dt$$

$$= (A_1 A_2/2)\cos(\alpha_1 - \alpha_2). \qquad (11)$$

If we use the modulating current shown in Fig. 2(c), and sample-and-hold the interference signal at times t_i and t_j the end of the fraction of the modulating current indicated in Fig. 2(c), we can obtain two interference signals $S_1(t_i)$ and $S_2(t_j)$ at the same time, where i and j are integers. Then the self-correlation can be calculated in real time.

3. EXPERIMENTAL SETUP

In the experimental setup shown in Fig. 1, the central wavelength λ_0, maximum output power, and modulation efficiency β are 780 nm, 10 mW, and 7.43×10^{-3} nm/mA, respectively. The object mirror is mounted on an x-axis stage. The optical path difference $2D_0$ is 210 mm.

The block diagram of the MSG is shown in Fig. 3. The frequency f of the rectangular oscillator (OSC), which is used to generate the modulating signal, is 1 MHz. This same frequency is used to sample the interference signals. The rectangular signal is divided into 1/200, by dividers (DIV1 and DIV2) and is then fed to an integrator (INT), which converts the rectangular signal to a triangular one. Therefore, the frequency of the triangular modulating signal becomes 5 kHz. The bias circuit (BIAS) then adds the dc bias signal to this triangular signal. The two triangular modulating signals, one of which has a dc bias, are fed to the analog switch (ASW). If only the upper contact in the ASW is always closed, the normal

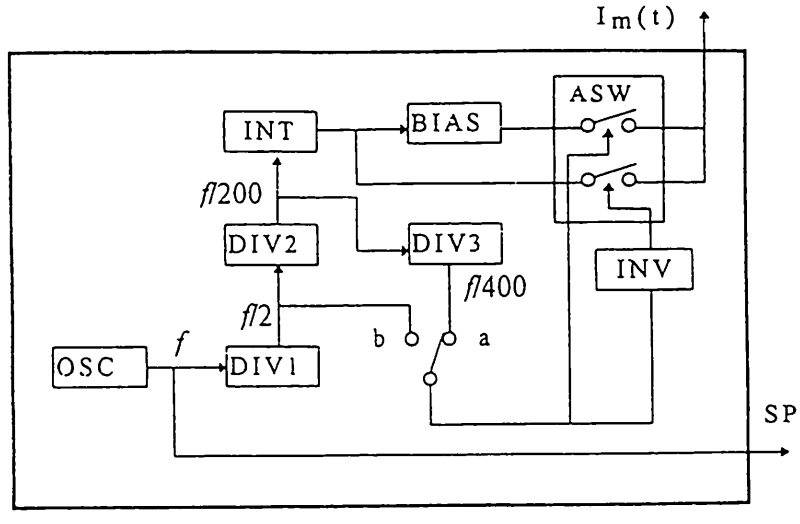

Fig. 3 Block diagram of the modulation signal generator MSG.

modulating signal shown in Fig. 2(a) is obtained. The timing of the switching is controlled by the output of DIV1 or DIV3. The change of the switching signal is made by a mechanical switch. When the contact is closed at side-a, it offers us the high-speed time-shared modulating signal shown in Fig. 2 (c), because the frequency of the output of DIV1 is $f/2$ or 500 kHz. On the other hand, when the contact is closed at side-b, the DIV3 whose output frequency is $f/400$ or 2.5 kHz is used, and we can obtain the time-shared modulating signal shown in Fig. 2(b).

4. EXPERIMENTAL RESULTS

We implemented several heterodyne modulations using the three kinds of modulating signals shown in Fig. 2. In these experiments, the frequency of the triangular modulating signal and the rate of current modulation were 5 kHz and 6 mA/ms, respectively.

First, the normal heterodyne modulation shown in Fig. 2(a) was carried out. The S(t) was obtained, as shown in Fig. 4.

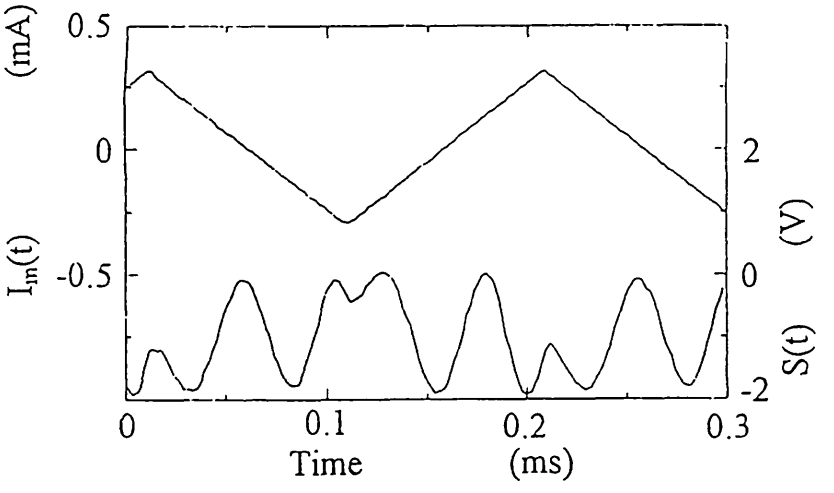

Fig. 4 Interference signal in the normal heterodyne modulation

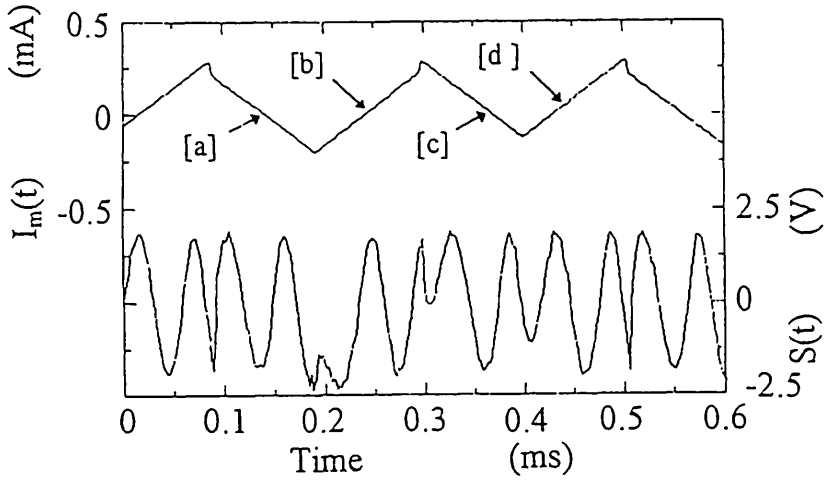

Fig. 5 The S(t) in the time-shared heterodyne modulation

The upper trace is the modulating current and lower one is the S(t). It changes sinusoidally, as described in Eq. (3), but it was noticed to have a short time-delay at the point where the inclination of modulating current changed.

Next, we carried out the time-shared modulation shown in Fig. 2(b). The bias current superimposed on sections [c] and [d] of the triangular current was 0.076 mA. The S(t) obtained is shown in Fig. 5. If the frequency of S(t) is same among all four sections [a] to [d], the approximation of $\omega_{c1}=\omega_{c2}$ is held and Eq. (10) is applicable. We measured the frequency of the S(t) at sections [a] to [d] to confirm the that approximation. We adjusted the rate of current modulation, or the inclination of the modulating current, and calculated the frequency by means of standard FFT analysis. The results shown in

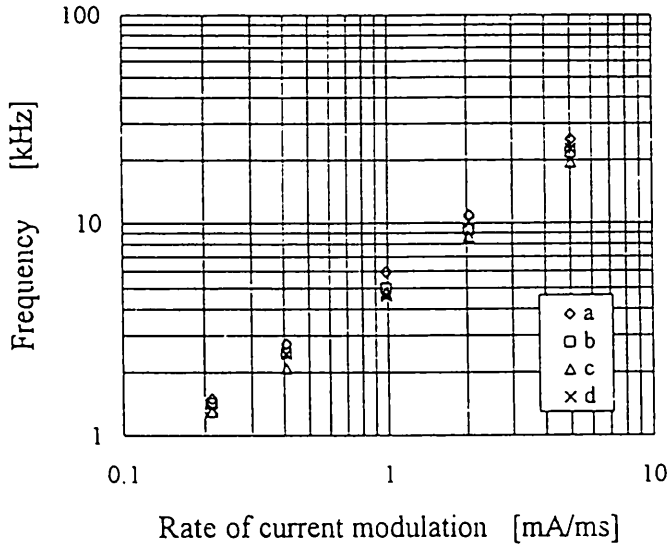

Fig. 6 Measured frequencies of the S(t)

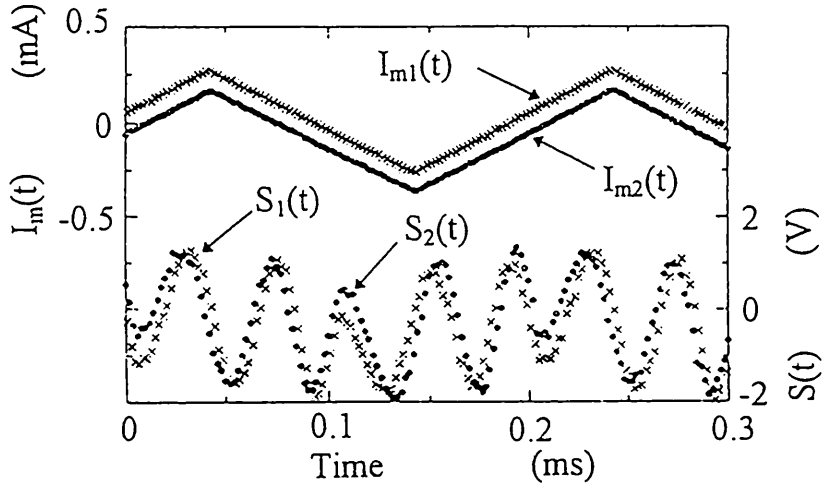

Fig. 7 The S(t) in the high-speed time-shared heterodyne modulation

Fig. 6 indicate how the frequencies in sections [b] and [d] are nearly the same, but those in the sections [a] and [c] vary somewhat from those in sections [b] and [d]. The difference in frequency of S(t) is caused by a delay of the wavelength's change in the LD. In this time, the wavelength's change does not follow the modulating current. So, we can use the interference signals in sections [b] and [d], and the self-correlation function ρ can be calculated by using Eq. (11). The difference of the phase was then calculated as $\Delta\alpha$=2.428 rad, and the absolute distance was calculated as 209.02 mm.

Finally, the high-speed time-shared modulation shown in Fig. 2(c) was carried out. The result is shown in Fig. 7. The time-shared modulating currents $I_{m1}(t)$ and $I_{m2}(t)$ are represented by alternating crosses and dots. Since the switching frequency was 500 kHz, the interval of the time t_i and t_j in Fig. 2(c) was 1 μs. The interference signals $S_1(t)$ and $S_2(t)$ are also represented by crosses and dots, which correspond to those of $I_{m1}(t)$ and $I_{m2}(t)$. The phase difference was detected between the $S_1(t)$ and the $S_2(t)$, and it was calculated as 0.80 rad. Then the absolute distance was calculated as 68.87 mm. It is rather shorter than that had been expected. It is therefore considered that the wavelength is unable to fluctuate at the speed with which the modulating current switches. If the detected phase difference is correct, the modulation efficiency β is calculated as 2.43×10^{-3} nm/mA. This is about one-third of the β which is obtained in the normal heterodyne modulation. Therefore, we have to estimate the effective modulating efficiency of the LD under high-speed phase modulation to achieve the real-time distance measurement accurately.

4. CONCLUSION

We have proposed a new type of TWI for an absolute measurement of distance, in which the time-shared phase modulation is utilized. Since it uses one LD to obtain two different wavelengths, the construction of an optical system is made easy. The self-correlation function is used for the phase detection between two kinds of interference signals, therefore, also signal processing is simple and accurate. If the high-speed time-shared modulation is used, two different phase-shifted interference signals are obtained simultaneously. Using our method, there is a possibility of the real-time and accurate distance measurement.

ACKNOWLEDGMENTS

We thank Mr. Kendall J. T. Walls for his help with the revision of this paper. This work was supported by a scientific research grant (No. 08750508) from the Ministry of Education in Japan.

6. REFERENCES

1) T. Yoshino, M. Nara, S. Mnatzakanian, B. S. Lee, and T. C. Strand, "Laser diode feedback interferometer for stabilization and displacement measurement," *Appl. Opt.* **26**, 892-897 (1987).

2) O. Sasaki, K. Takahashi, and T. Suzuki, "Sinusoidal phase modulating laser diode interferometer with a feedback control system to eliminate external disturbance," *Opt. Eng.* **29**(12), 1511-1515 (1990).

3) I. Yamaguchi, J. Liu, J. Kato, "Active phase-shifting interferometers for shape and deformation measurements," *Opt. Eng.* **35**(10), 2930-2937 (1996).

4) T. Suzuki, T. Okada, O. Sasaki, and T. Maruyama, "Feedback type of laser diode interferometer with an optical fiber," *Proc. SPIE* **2860**, 225-231 (1996).

5) M. Takeda, and T. Abe, "Phase unwrapping by a maximum cross amplitude spanning tree algorithm: a comparative study," *Opt. Eng.* **35**(8), 2345-2351 (1996).

6) J. C. Wyant, "Testing aspherics using two-wavelength holography," *Appl. Opt.* **10**, 2113-2118 (1971).

7) A. F. Fercher, H. Z. Hu, and U. Vry, "Rough surface interferometry with a two-wavelength heterodyne speckle interferometer," *Appl. Opt.* **24**, 2181-2188 (1985).

8) Y.-Y Cheng and J. C. Wyant, "Two-wavelength phase shifting interferometry," *Appl. Opt.* **23**, 4539-4543 (1984).

9) K. Creath, " Step height measurement using two-wavelength phase-shifting interferometry," *Appl. Opt.* **26**, 2810-2816 (1987).

10) A. J. den Boef, "Two-wavelength scanning spot interferometer using single-frequency diode lasers," *Appl. Opt.* **27**, 306-311 (1988).

11) P. de Groot and S. Kishner, "Synthetic wavelength stabilization for two-color laser-diode interferometry," *Appl. Opt.* **30**, 4026-4033 (1991).

12) T. Suzuki, O. Sasaki, and T. Maruyama, "Phase-locked laser diode interferometry for surface profile measurement," *Appl. Opt.* **28**(20), 4407-4410 (1989).

13) T. Suzuki, O. Sasaki, K. Higuchi, and T. Maruyama, "Differential type of phase locked laser diode interferometer," *Appl. Opt.* **31**(34), 7242-7248 (1992).

14) T, Suzuki, T, Mutoh, O. Sasaki, and T. Maruyama, "Wavelength-multiplexed phase-locked laser diode interferometer using phase-shifting technique," *Appl. Opt.* (in press).